land

MDPI

Article

Determination of Contributing Area Threshold and Downscaling of Topographic Factors for Small Watersheds in Hilly Areas of Purple Soil

Ruiyin Chen [1,2,*,†], Yonggang Zhu [1,†], Jun Zhang [1], Anbang Wen [2], Shudong Hu [1], Jun Luo [1] and Peng Li [1]

[1] POWERCHINA Chengdu Engineering Corporation Limited, Chengdu 611130, China
[2] Institute of Mountain Hazards and Environment, Chinese Academy of Sciences, Chengdu 610041, China
* Correspondence: chenruiyin@imde.ac.cn; Tel.: +86-028-60753035
† These authors contributed equally to this work.

Abstract: The results of topographic factor computations are highly sensitive to the setting of contributing area thresholds when applied to soil erosion modeling to evaluate soil erosion; however, the existing choice of contributing area thresholds is highly arbitrary. Meanwhile, due to regional-scale limitations, lower-resolution DEM data are usually used to calculate topographic factors, and with the fragmentation of land parcels in hilly areas of purple soil, lower-resolution DEM data respond to very limited topographic information. This study focuses on solving the mentioned issues by selecting the Lizixi watershed in a hilly area of purple soil as the research subject. It establishes a relationship equation between the resolution of DEM data and the optimal contributing area threshold. This is achieved by investigating the change in the contributing area threshold with the resolution of DEM data, determining the optimal contributing area threshold for different resolutions of DEM data, and establishing the relationship equation between the resolution of DEM data and the optimal contributing area threshold. Meanwhile, to solve the key problem of fragmented land parcels in the purple soil area, where the low-resolution and medium-resolution DEM data cannot accurately reflect the topographic information, combined with the principle of histogram matching, the downscaling model between the topographic factors under the low-resolution DEM data and the topographic factors under the high-resolution DEM data is established. This study confirms that the scale transformation model developed has a strong simulation effect, and the findings can offer technical assistance for the precise computation of soil erosion in small watersheds in hilly areas of purple soil.

Keywords: hilly area of purple soil; contributing area threshold; DEM; topographic factors; downscaling

check for updates

Citation: Chen, R.; Zhu, Y.; Zhang, J.; Wen, A.; Hu, S.; Luo, J.; Li, P. Determination of Contributing Area Threshold and Downscaling of Topographic Factors for Small Watersheds in Hilly Areas of Purple Soil. *Land* **2024**, *13*, 1193. https://doi.org/10.3390/land13081193

Academic Editor: Wojciech Zgłobicki

Received: 17 June 2024
Revised: 31 July 2024
Accepted: 1 August 2024
Published: 2 August 2024

Copyright: © 2024 by the authors. Licensee MDPI, Basel, Switzerland. This article is an open access article distributed under the terms and conditions of the Creative Commons Attribution (CC BY) license (https://creativecommons.org/licenses/by/4.0/).

1. Introduction

The slope length (L) and steepness (S) factors are crucial for effectively assessing water erosion in China using the CSLE method. The slope length factor is determined by the slope length parameter, which is derived from the digital elevation model (DEM). The contributing area threshold is utilized to establish the endpoint of the slope length and the distribution of the river network when calculating the slope length parameter. If the contributing area exceeds the contributing area threshold, the grid is classified as a gully, and the slope length ends [1–3]. The contributing area refers to the area occupied by the cells where all water flows into this grid. The slope length factor is directly impacted by the contributing area threshold, which in turn affects the accuracy of the assessment of soil erosion. Currently, there is a limited number of studies available on identifying the optimal contributing area threshold.

When applying soil erosion models like USLE, RUSLE, and CSLE to study soil erosion across extensive areas, regional-scale constraints sometimes require the use of lower-resolution DEM data (30 m or less) for calculating the LS factor. Prior research has demon-

strated that this will result in slope attenuation and an elongation of the slope [4–9]. At the same time, DEM data with different resolutions contain different terrain information. The lower resolution of the DEM data contains more fuzzy terrain information, resulting in errors in the LS factor calculated by the low-resolution DEM. The LS factor plays a crucial role in soil erosion assessment, particularly in hilly areas of purple soil where fragmented plots and low-resolution DEM data provide limited topographic details. Choosing high-resolution DEM data is critical for precisely representing the study area's topography and calculating soil erosion results with precision. When the resolution of DEM data cannot meet the demand for high accuracy, it is necessary to scale the LS factor calculated by the medium- and low-resolution DEM data to obtain the LS factor calculated by the high-resolution DEM data. This is crucial for the evaluation of soil erosion [5,10].

The hilly purple soil region has comparatively few land resources. Additionally, the destruction of agricultural practices, production, and construction has made the region's ecological environment more fragile, increasing the risk of severe soil erosion and frequent localized mountain disasters. However, the topography of this region is fragmented, and the lower resolution of DEM data responds to limited topographic information, which seriously affects the accuracy of soil erosion evaluation. Therefore, this study is devoted to determining the optimal contributing area threshold and downscaling of topographic factors to improve the accuracy of soil erosion calculation in this region.

2. Materials and Methods

2.1. Study Area

Lizixi is one of the major tributaries of the middle reaches of the Jialing River, located in the central hilly area of the Sichuan Basin in China, with a watershed area of 425 km^2. The latitude and longitude of the watershed is between 30°22′ and 30°42′ N and 105°47′ and 106°06′ E, and the latitude and longitude of the watershed control station is 105°59′15″ E and 30°32′44.002″ N (Figure 1). The region is a humid subtropical climate zone with abundant rainfall and four distinct seasons, with a multi-year average temperature of 17.4 °C. With elevations varying from 222 m to 503 m above sea level, the watershed's topography is undulating, high in the north and low in the south. The majority soil type in the watershed is purple soil. Dryland and forested land are the main types of land use in the watershed, with dry land accounting for 36.70% of the total watershed area and forested land accounting for 31.33% of the total watershed area. The natural environment of this watershed is representative of a hilly area of purple soil [11,12].

2.2. Experimental Procedure

In this study, by analyzing the relationship between the contributing area threshold and the resolution of DEM data, we then use the mean change-point analysis method to identify the optimal contributing area threshold for various resolutions of DEM data. Finally, we establish an equation that relates the resolution of DEM data to the optimal contributing area threshold. The scale transformation of the LS factor derived at low and medium resolutions is performed based on an analysis of the terrain factors' scale influence and the idea of histogram matching (Figure 2).

2.3. Base Datasets

The primary input data for this study consist of DEM data with varying resolutions. Obtaining contour lines and elevation points from a 1:5000 topographic map of the research area, we then create DEM data at various resolutions (2.5, 5, 7.5, 10, 15, 20, 25, 30, 35, 40, 45, 50, 55, 60, 65, 70, 75, 80, 85, 90 m) through the AUNDEM algorithm by combining vector data such as the boundary of the study area, rivers, and lakes. Soil erosion is calculated by the CSLE model, which consists of rainfall erosivity factor R, soil erodibility factor K, slope length factor L, slope gradient factor S, vegetation cover and biological measures factor B, engineering measures factor E, and tillage measures factor T. The specific calculation method of each factor and related data sources refer to previous literature [13].

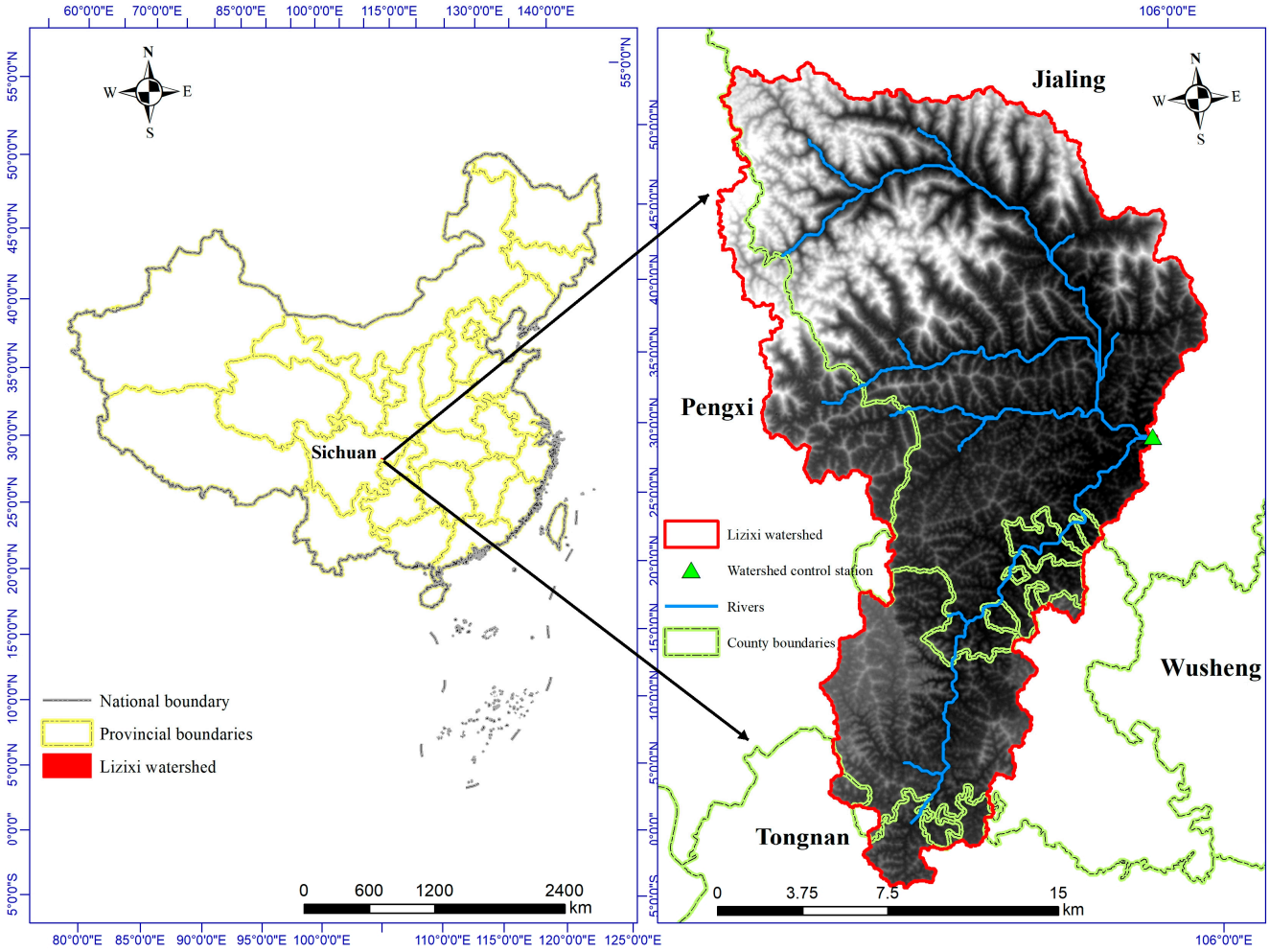


Figure 1. Location of Lizixi watershed.

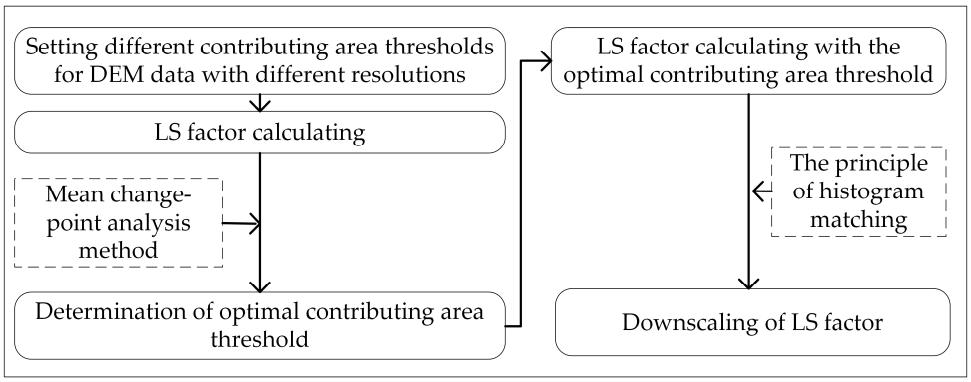


Figure 2. The technical roadmap.

2.4. Setting of Contributing Area Threshold

Based on the DEM data at 2.5, 5, 7.5, 10, 15, 20, 25, 30, 35, 40, 45, 50, 55, 60, 65, 70, 75, 80, 85, and 90 m resolution of the Lizixi watershed, the contributing area thresholds are set to 10, 15, 20, 25, 30, 50, 70, 90, 110, 130, 150, 200, 500, 1000, 2000, and 5000 rasters, respectively, to calculate the corresponding topographic parameters. In this study, the topographic parameters were calculated concerning previous studies [14,15].

2.5. Determination of Optimal Contributing Area Threshold

The mean change-point analysis method is based on statistical principles to judge and test the existence of change points and determine one or more change points [16]. The purpose of using this method is to determine the optimal advantage of a curve changing from steep to gentle through data analysis [17]. The results of existing studies have demonstrated the high feasibility and credibility of the methodology [18,19]. The mean change-point analysis method is a mathematical–statistical method of working with nonlinear data, which is calculated as follows:

(1) Let i = 2,. . ., N, for each i divide the sample into two segments: X_1, X_2, X_{i-1}, and X_i, X_{i+},. . .,X_N. Calculate the arithmetic mean X_{i1} and X_{i2} of the samples in each segment, and the statistic S_i, as follows.

$$S_i = \sum_{t=1}^{i-1} \left(X_t - \overline{X}_{i1}\right)^2 + \sum_{t=1}^{N} \left(X_t - \overline{X}_{i2}\right)^2 \quad (1)$$

(2) Calculate the statistic as follows.

$$\overline{X} = \sum_{t=1}^{N} \frac{X_t}{N} \quad (2)$$

$$S = \sum_{t=1}^{N} \left(X_t - \overline{X}\right)^2 \quad (3)$$

(3) Calculate the expected value E($S - S_i$), i = 2, 3,. . ., N. Among them, S is the statistical measure of the original sample, and S_i is the statistical measure of the segmented sample. When the E is the highest in the current period, the corresponding threshold is the optimal contributing area threshold. The calculation formula is as follows:

$$\mathrm{E}(S - S_i) = \mathrm{E}\frac{(i-1) \times (N-i+1) \times \left(\overline{X}_{i1} - \overline{X}_{i2}\right)^2}{N} \quad (4)$$

2.6. Downscaling of LS Factor

The principle of histogram matching refers to the transformation enhancement of image information by transforming the histogram of a certain image into the histogram of the target image through certain mathematical models [20]. In this study, we apply the method to the scale transformation of LS factors, so that the LS factors computed by low-resolution DEM can also effectively express the LS factors computed under high-resolution DEM.

The cumulative frequency plots of the original and target images are shown in Figure 3. The process of histogram matching goes as follows: first, the cumulative frequency A(X_1, Y) corresponding to an arbitrary factor value C(X_1, 0) is read from the original image's cumulative frequency curve. Next, the target image's cumulative frequency curve yields the factor value D(X_2, Y), which corresponds to the cumulative frequency B(X_2, Y). The factor value B(X_2, Y) of the original image is then corrected through the factor value D(X_2, Y) of the target image to realize the factor scale transformation (the red arrow in Figure 3). The specific steps are as follows:

(1) LS factor cumulative frequency histogram export: based on the GIS platform to count the factor frequency table in each DEM resolution, we then calculate its cumulative frequency percentage.

(2) LS factor correction: the target image is the factor calculated by the 2.5 m DEM. For the convenience of calculation, the cumulative frequency function f(x) of the target image is firstly fitted, and then the cumulative frequency calculated by the original image is used as the dependent variable Y, which is brought into the function to find the correction value X. The LS factor is calculated by the original image.

(3) Downscaling modeling: Plotting the factor and factor-corrected value curves, we then fit the factor downscaling model.

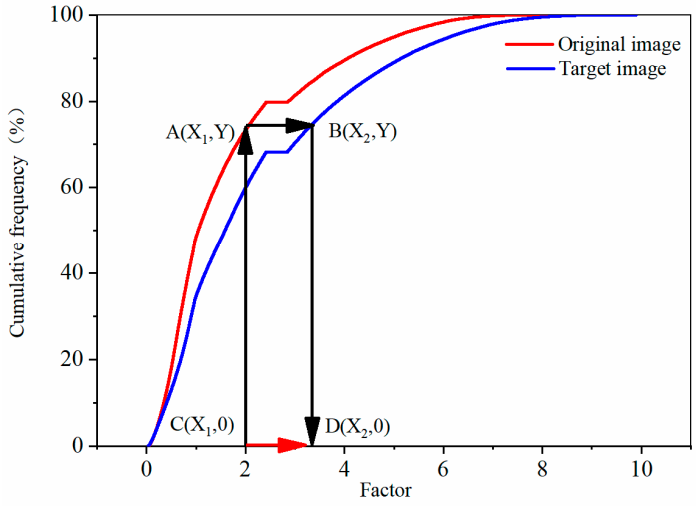


Figure 3. Schematic diagram of the histogram matching principle.

3. Results

3.1. Optimal Contributing Area Threshold

Figure 4 illustrates the pattern of change in the LS factor's mean value with respect to the contributing area threshold in the study area at various resolutions. When using DEM as a data source to calculate the slope length, it is necessary to determine the gullies first, and the extraction of the gullies is controlled by the contributing area threshold. In the current research results, determining the optimal contributing area threshold is mostly based on the relationship between river network density and contributing area threshold. The core idea is to take the contributing area threshold corresponding to the stabilization of the changing areas of the river network density as the optimal value [17,18,21,22]. As can be seen from Figure 4, the LS factor determined by the DEM at each resolution exhibits a tendency to increase and then gradually stabilize. Combining the results of previous studies [17,18,21,22], in this study, the optimal contributing area threshold is the one that corresponds to the stabilization of the LS factor.

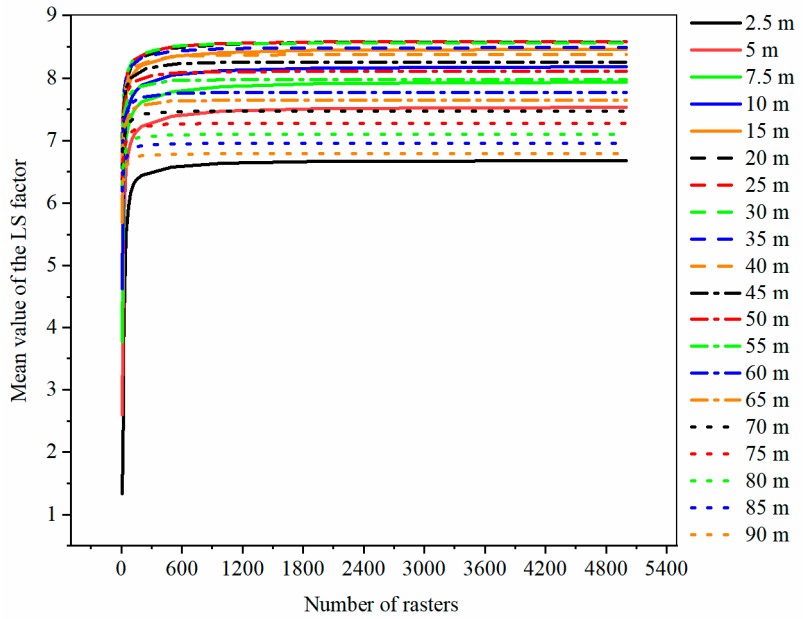


Figure 4. Pattern of change in the mean value of the slope length factor with contributing area threshold in the study area at different resolutions.

From the calculation results of the optimal contributing area threshold (Figure 5), it can be seen that the optimal contributing area threshold corresponding to the LS factor tends to increase completely with the decrease in the DEM resolution, and based on this law, the relationship equation between the DEM resolution and the optimal contributing area threshold was formulated in this study as follows:

$$y = 49.76475x^{2.00109} \quad r^2 = 0.99998, \; p < 0.01 \tag{5}$$

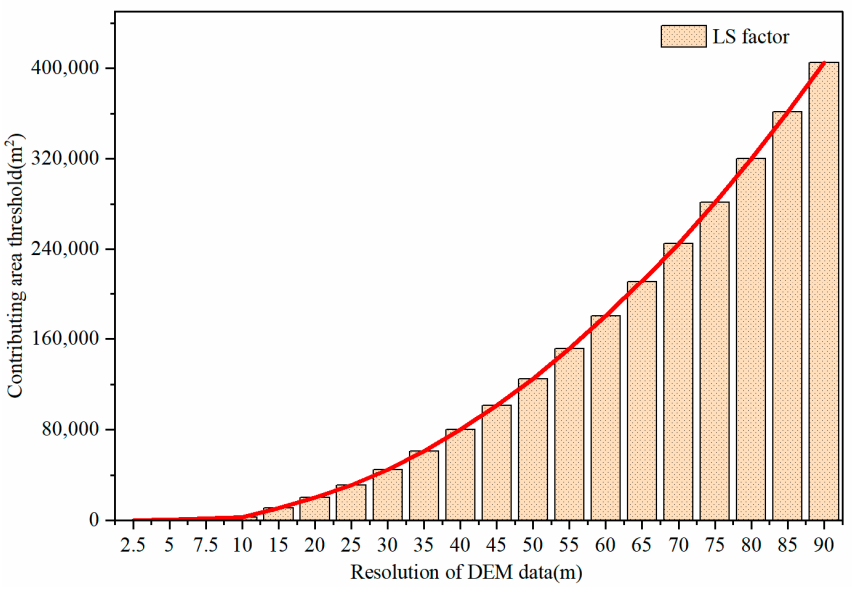


Figure 5. Optimal contributing area thresholds corresponding to LS factors at different resolutions of the DEM.

The DEM data resolution is denoted by x, while the ideal contributing area threshold is represented by y.

3.2. LS Factor Scale Effects

The statistical eigenvalues of slopes from the DEM data with varying resolutions show that as the resolution decreases, the mean slope value decreases (Figure 6). Additionally, the range between the maximum and minimum slope values decreases gradually, indicating a concentration of slope values. The lowest-resolution DEM data show a 50% reduction in both the mean slope value and the difference between the maximum and minimum slope values compared to the highest-resolution DEM data.

The rate of change in the mean is the value of the change in the mean caused by a change in unit resolution. The rate of change in the standard deviation is the value of the change in the standard deviation caused by a change in unit resolution. The specific calculations are based on the following formula [10]:

$$R_1 = |\frac{M_a - M_b}{a - b}| \tag{6}$$

$$R_2 = |\frac{S_a - S_b}{a - b}| \tag{7}$$

where R_1 is the rate of change in the mean value, M_a is the mean value of the slope/slope length/LS factor calculated by the higher-resolution DEM data, M_b is the mean value of the slope/slope length/LS factor calculated by the lower-resolution DEM data, R_2 is the rate of change in the standard deviation, S_a is the standard deviation of the slope/slope length/LS factor/calculated by the higher-resolution DEM data, and S_b is the standard deviation of the slope/slope length/LS factor calculated by the lower-resolution DEM data, with a being the higher-resolution value and b being the lower-resolution value. In this

study, the larger the value of R_1 or R_2, the more drastic is the change in slope/length/LS factor with the resolution of DEM data.

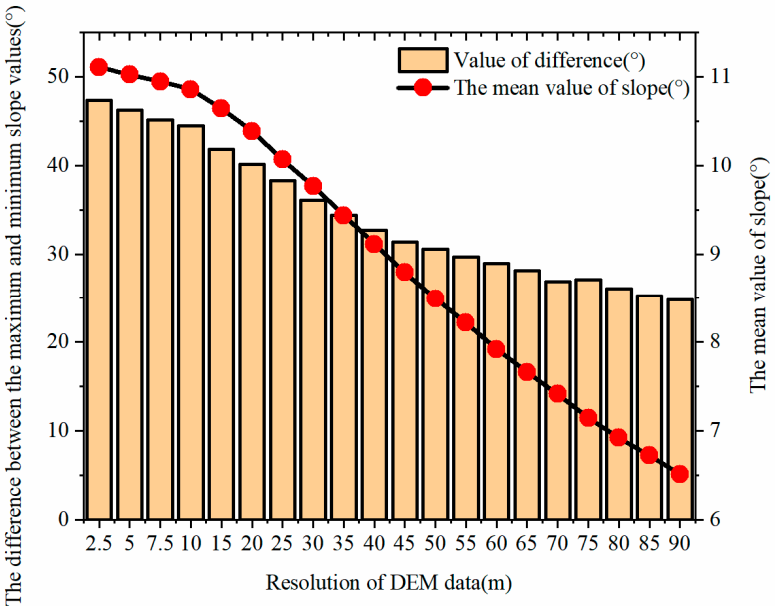


Figure 6. Statistical eigenvalues of slopes with different DEM resolutions.

The slope mean difference, mean change rate, standard deviation difference, and standard deviation change rate all show a tendency of increasing first and then decreasing (Table 1 and Figure 7). The slope attenuation in this interval is drastic, and the slope value changes are large when the resolution of the DEM data is between 0 and 35 m. Conversely, when the accuracy of the DEM data decreases between 35 and 90 m, the slope attenuation in this interval is small, and the slope value data are more aggregated. However, the fact is that the topography of the Lizixi watershed is undulating, and the slope varies greatly within the watershed [12]. It shows that the DEM data's resolution significantly distorts the slope values at 35 to 90 m, and thus calculating slopes directly from the low-resolution DEM data has poor accuracy and has to be improved.

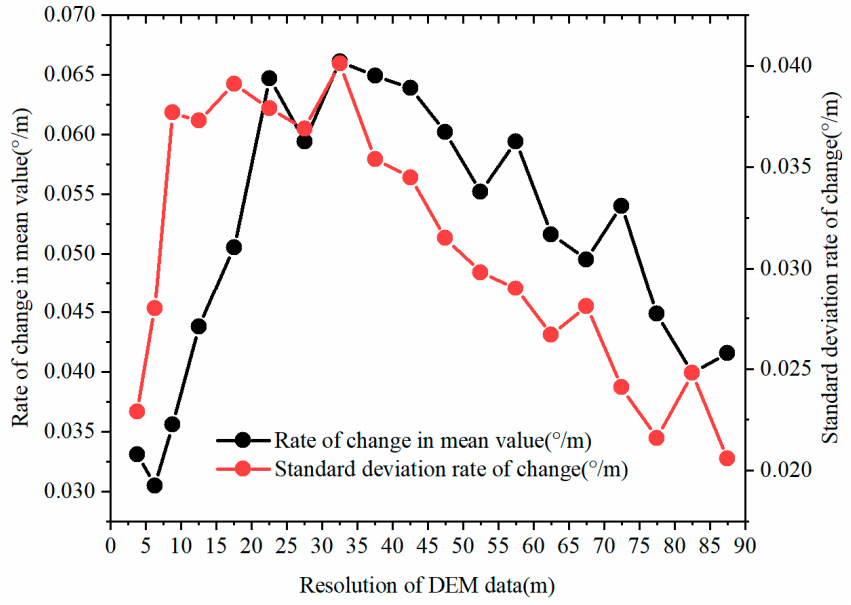


Figure 7. Rate of change in the mean and standard deviation of slope.

Table 1. Mean and standard deviation of slope.

DEM Resolution Change Interval (m)	Mean Difference	R_1	Difference in Standard Deviation	R_2
2.5–5	0.0828	0.0331	0.0573	0.0229
5–7.5	0.0764	0.0305	0.0699	0.0280
7.5–10	0.0889	0.0356	0.0942	0.0377
10–15	0.2189	0.0438	0.1867	0.0373
15–20	0.2523	0.0505	0.1957	0.0391
20–25	0.3234	0.0647	0.1896	0.0379
25–30	0.2971	0.0594	0.1845	0.0369
30–35	0.3304	0.0661	0.2007	0.0401
35–40	0.3245	0.0649	0.1769	0.0354
40–45	0.3194	0.0639	0.1725	0.0345
45–50	0.3012	0.0602	0.1577	0.0315
50–55	0.2761	0.0552	0.1492	0.0298
55–60	0.2969	0.0594	0.1451	0.0290
60–65	0.2578	0.0516	0.1336	0.0267
65–70	0.2473	0.0495	0.1405	0.0281
70–75	0.2701	0.0540	0.1205	0.0241
75–80	0.2243	0.0449	0.1079	0.0216
80–85	0.1994	0.0399	0.1240	0.0248
85–90	0.2081	0.0416	0.1032	0.0206

The slope length value is gradually becoming more discrete as the resolution of the DEM data decreases. This is indicated by the mean slope length value showing an increasing trend and the gradual increase in the difference between the maximum and minimum slope length values. The lowest-resolution DEM data increase about seven times compared with the slope length mean value corresponding to the highest-resolution DEM data, while the difference between the maximum slope length value and the minimum slope length value increases about 32 times (Figure 8).

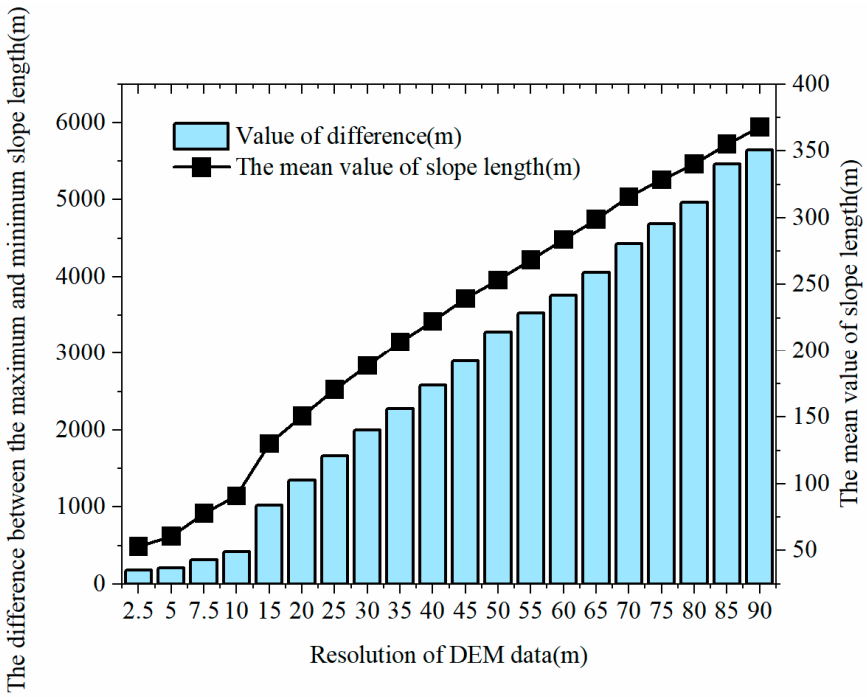


Figure 8. Statistical eigenvalues of slope length corresponding to DEM data with different resolutions.

Table 2 and the Figure 9 show that the absolute value of the difference in the mean value of the slope length, the rate of change in the mean value, the absolute value of the difference in the standard deviation, and the rate of change in the standard deviation have a propensity to rise initially before falling. When the DEM data resolution falls between 0 and 15 m, the slope length's R_1 and R_2 increase as the resolution of the DEM data decreases. However, when the resolution of the DEM data falls between 15 and 90 m, the R_1 and R_2 show a decreasing trend as the DEM data's resolution decreases, and the magnitude of the decrease gradually becomes smaller and tends to level off.

Table 2. Mean and standard deviation of slope length.

DEM Resolution Change Interval (m)	Mean Difference	R_1	Difference in Standard Deviation	R_2
2.5–5	−7.9104	3.1642	−8.6227	3.4491
5–7.5	−16.9142	6.7657	−13.5297	5.4119
7.5–10	−13.0468	5.2187	−12.0668	4.8267
10–15	−39.2214	7.8443	−53.9863	10.7973
15–20	−20.6984	4.1397	−32.1550	6.4310
20–25	−19.7499	3.9500	−29.8419	5.9684
25–30	−18.0244	3.6049	−27.3635	5.4727
30–35	−17.9251	3.5850	−24.8265	4.9653
35–40	−15.8052	3.1610	−22.2297	4.4459
40–45	−17.0631	3.4126	−23.6329	4.7266
45–50	−13.7633	2.7527	−17.4191	3.4838
50–55	−15.3524	3.0705	−20.9577	4.1915
55–60	−15.1956	3.0391	−22.2281	4.4456
60–65	−15.1077	3.0215	−22.4376	4.4875
65–70	−16.9433	3.3887	−24.3855	4.8771
70–75	−12.5555	2.5111	−13.2517	2.6503
75–80	−12.0002	2.4000	−16.4137	3.2827
80–85	−14.7402	2.9480	−14.7272	2.9454
85–90	−12.9160	2.5832	−17.0352	3.4070

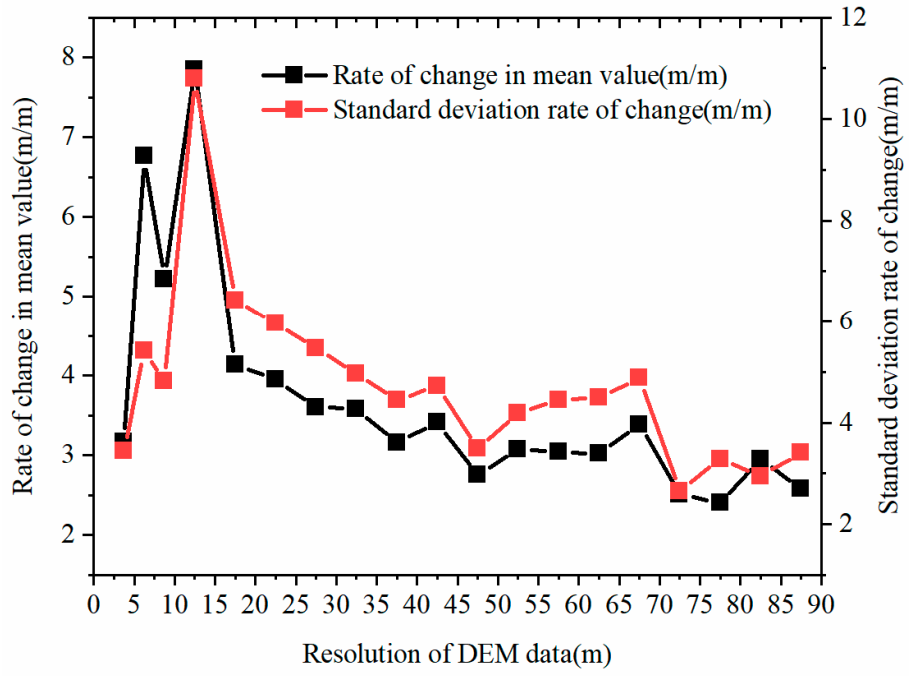


Figure 9. Rate of change in the mean and standard deviation of slope length.

The two rate-of-change curves show that the effect of the decreasing resolution of DEM data on slope length expansion decreases gradually with decreasing resolution. The results of earlier research are in line with this viewpoint [5,10,23].

The mean value of the LS factor and the gap between the maximum and minimum values exhibit an initial increasing and then declining pattern in response to the decline in the accuracy of the DEM data (Figure 10).

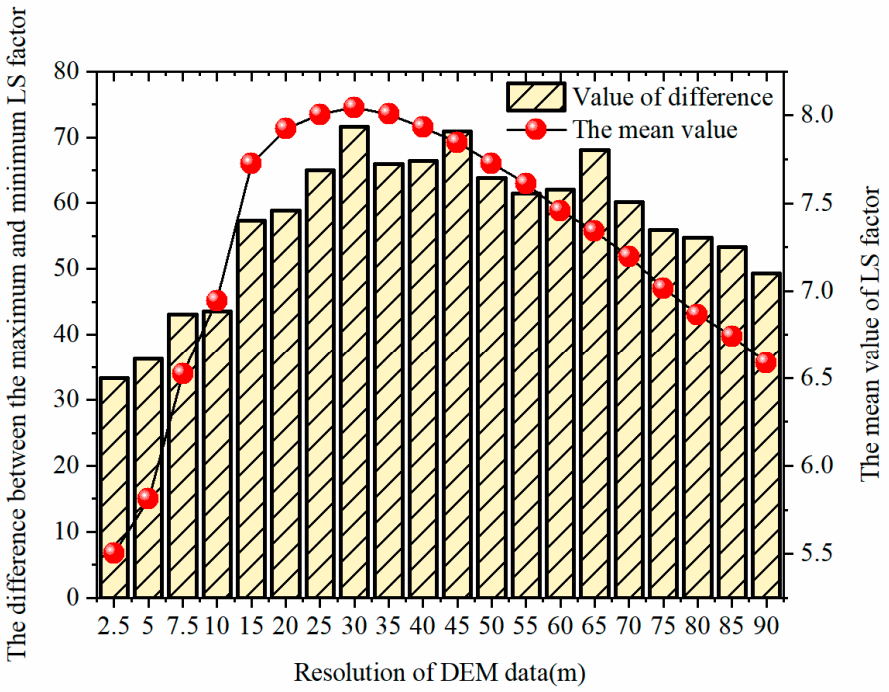


Figure 10. Statistical eigenvalues of LS factor corresponding to DEM data with different resolutions.

It can be seen that the LS factor mean difference, mean change rate, difference in standard deviation, and standard deviation change rate show a tendency of increasing and then decreasing (Table 3 and Figure 11). In the case of DEM data resolutions ranging from 0 to 7.5 m, both R_1 and R_2 show an increase with decreasing resolution, suggesting a significant change in the LS factor and large differences in LS factor values. In contrast, when DEM data resolutions range from 7.5 m to 90 m, R_1 and R_2 show a decrease with decreasing resolution, suggesting a smaller degree of LS factor changes in this interval and more aggregated LS factor values, while the LS factor changes eventually flatten out as DEM data precision declines.

According to the calculation method of CSLE factors, rainfall erosivity factor R, soil erodibility factor K, vegetation coverage and biological measures factor B, soil and water conservation engineering measures factor E, tillage measures factor T, and the LS factors are calculated by DEM data with different resolutions and then are substituted into the CSLE model to calculate the soil erosion modulus. According to the Classification and Grading Standards for Soil Erosion [24], the soil erosion results in the Lizixi watershed were obtained. As can be seen in Figure 12, regardless of either high- or low-accuracy DEM data, mild erosion dominated the soil erosion results in the Lizixi watershed, followed by moderate erosion, while intense erosion accounted for the smallest area. As DEM accuracy declines, the moderate erosion area exhibits a decreasing and then increasing and then decreasing trend, with a turning point at DEM 7.5 m and 20 m, respectively; the intense erosion area exhibits an increasing and then decreasing trend, with a turning point at DEM 20 m. The mild erosion area shows a trend of increasing and then decreasing and then increasing. There is a turning point at DEM 40 m for the region of highly intense erosion, which exhibits an overall trend of growing and then reducing, while the area of severe erosion displays an overall trend of declining and then increasing. The overall erosion area

showed a tendency of increasing and then reducing, with the maximum area attained at DEM 30 m. There was a growing and then declining trend in the severely eroded area, with the turning point at DEM 55 m. A map of the distribution of soil erosion intensity at different DEM resolutions (Figure 13) shows that high-intensity erosion in the Lizixi watershed is concentrated in the northern portion of the watershed, with some correlation to the distribution of LS factors.

Table 3. Mean and standard deviation of LS factor.

DEM Resolution Change Interval (m)	Mean Difference	R_1	Difference in Standard Deviation	R_2
2.5–5	−0.3109	0.1244	−0.4292	0.1717
5–7.5	−0.7108	0.2843	−0.5190	0.2076
7.5–10	−0.4214	0.1686	−0.3080	0.1232
10–15	−0.7791	0.1558	−0.5929	0.1186
15–20	−0.1994	0.0399	−0.2144	0.0429
20–25	−0.0815	0.0163	−0.1591	0.0318
25–30	−0.0396	0.0079	−0.1130	0.0226
30–35	0.0379	0.0076	−0.0360	0.0072
35–40	0.0736	0.0147	−0.0243	0.0049
40–45	0.0876	0.0175	−0.0105	0.0021
45–50	0.1193	0.0239	0.0158	0.0032
50–55	0.1143	0.0229	0.0144	0.0029
55–60	0.1538	0.0308	0.0277	0.0055
60–65	0.1170	0.0234	0.0292	0.0058
65–70	0.1441	0.0288	0.0815	0.0163
70–75	0.1820	0.0364	0.0676	0.0135
75–80	0.1491	0.0298	0.0727	0.0145
80–85	0.1244	0.0249	0.0803	0.0161
85–90	0.1540	0.0308	0.0751	0.0150

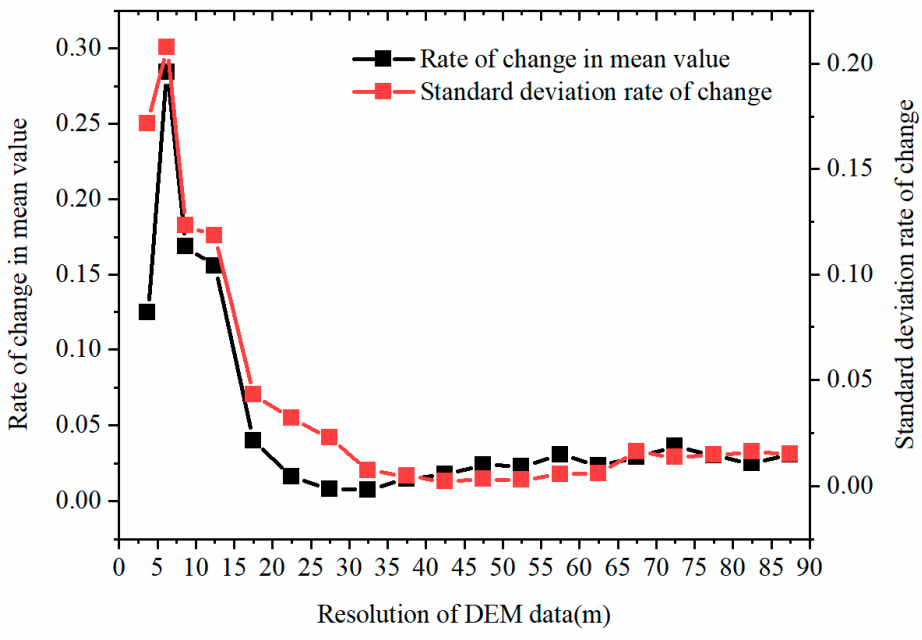


Figure 11. Rate of change in the mean and standard deviation of LS factor.

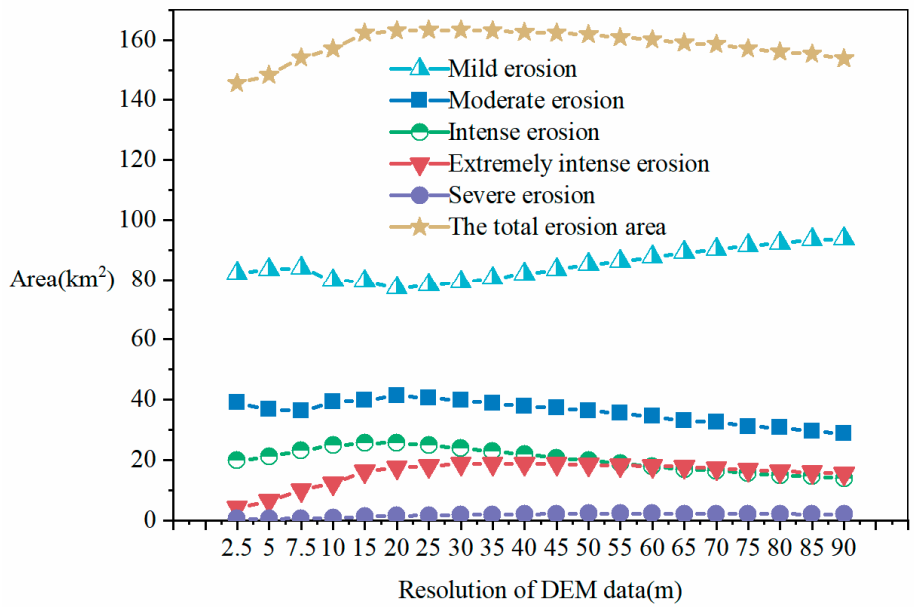


Figure 12. The area of soil erosion intensity varies with the resolution of DEM data.

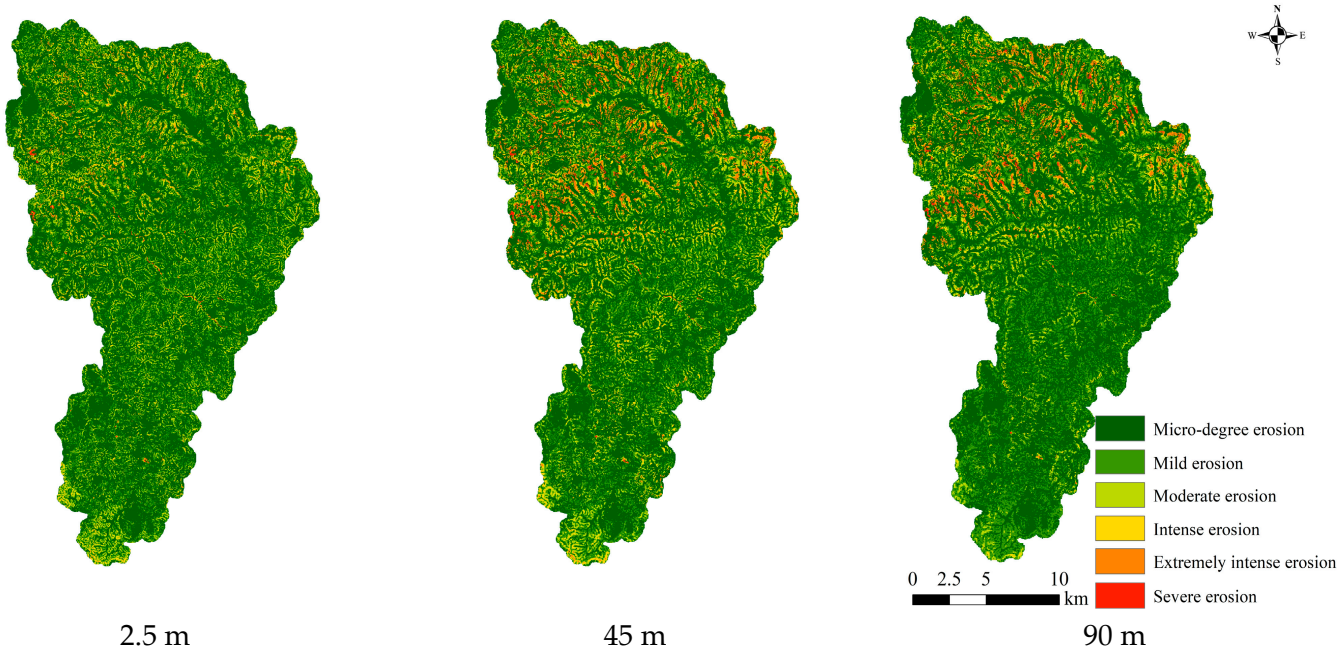


Figure 13. Distribution of soil erosion intensity at different resolutions of DEM data.

From the difference between the soil erosion area calculated by the low-resolution DEM data and the soil erosion area calculated by the 2.5 m high-resolution DEM data, Figure 14 illustrates how the difference in erosion area exhibits an increasing and subsequently declining trend as the precision of the DEM data decreases. Among them, the smallest erosion area difference is 5 m DEM, and the area difference is only 2.68 km^2, while the largest area difference is 30 m DEM, and the area difference is 17.66 km^2. The watershed area of the Lizixi watershed is 425 km^2, and the largest area difference has reached 4.16% of the watershed area.

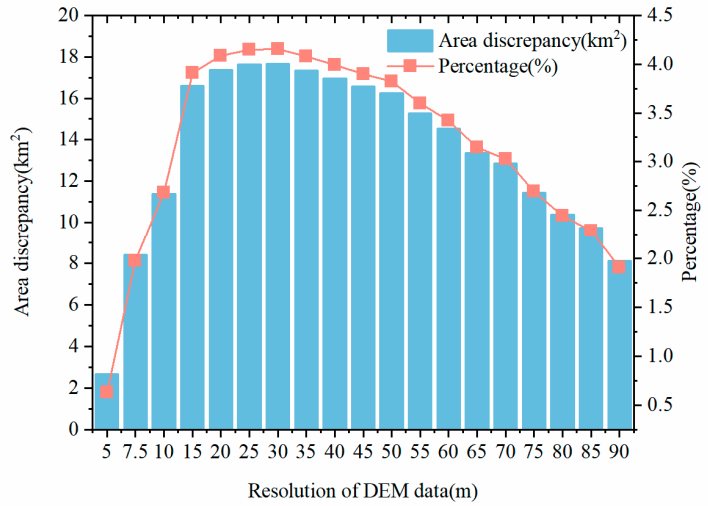


Figure 14. Difference in erosion area corresponding to low- and high-resolution DEM data.

3.3. Downscaling of LS Factor

The LS factor calculated by 2.5 m DEM data is taken as the target, and the LS factor calculated by other low-resolution DEM data is downscaled. According to the histogram matching principle, the LS factor downscaling model at 19 resolutions is obtained, as shown in Figure 15, and it can be seen that the model fits well, with R^2 above 0.99.

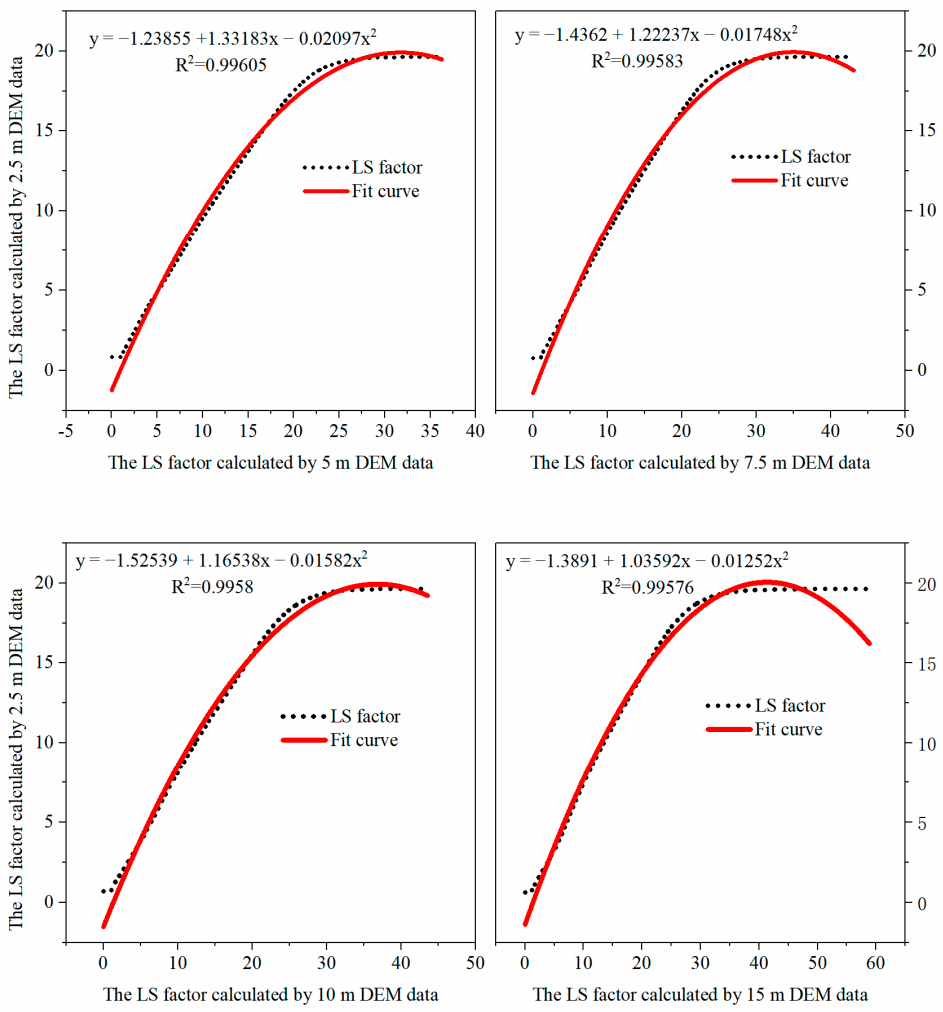


Figure 15. *Cont.*

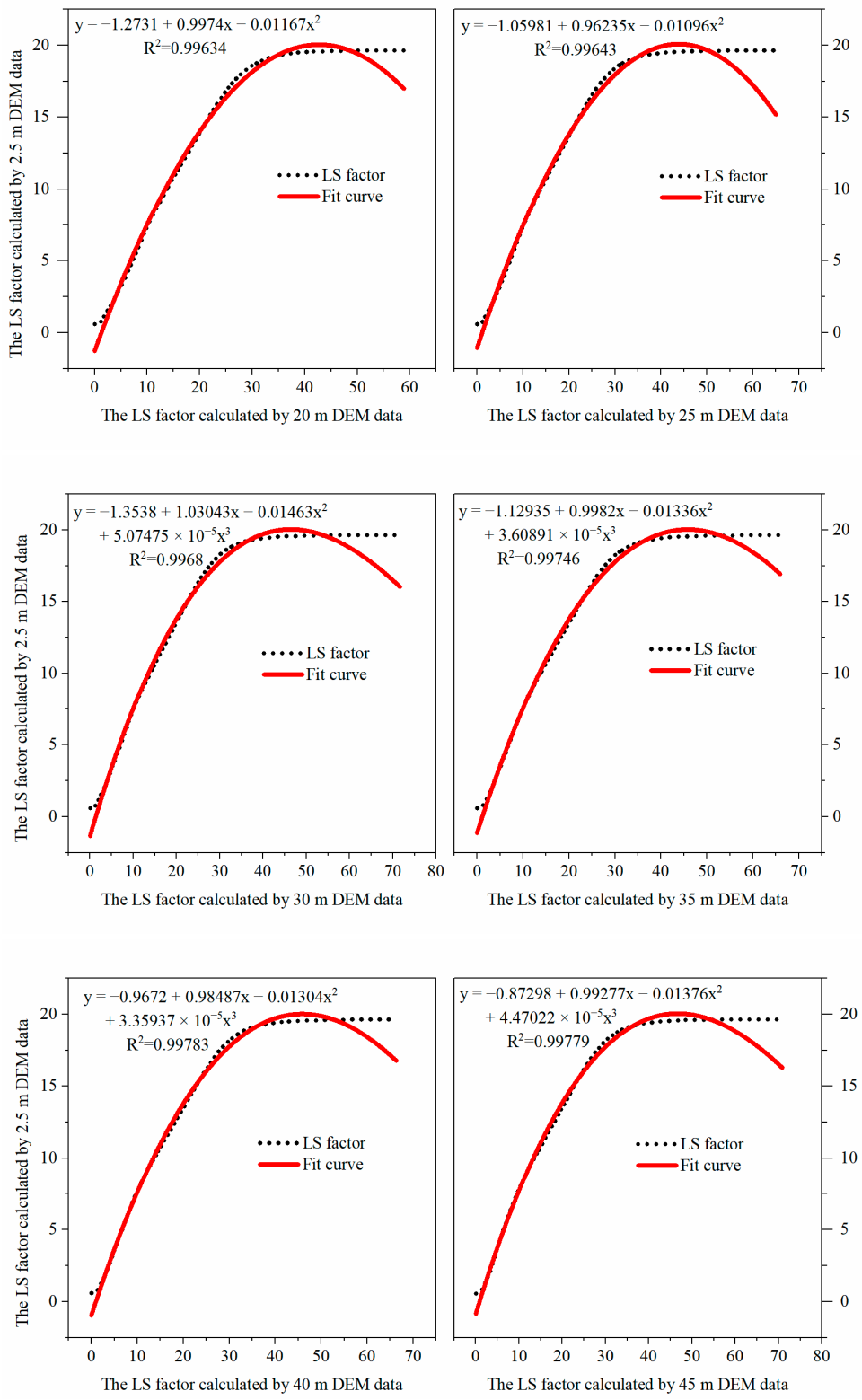


Figure 15. *Cont.*

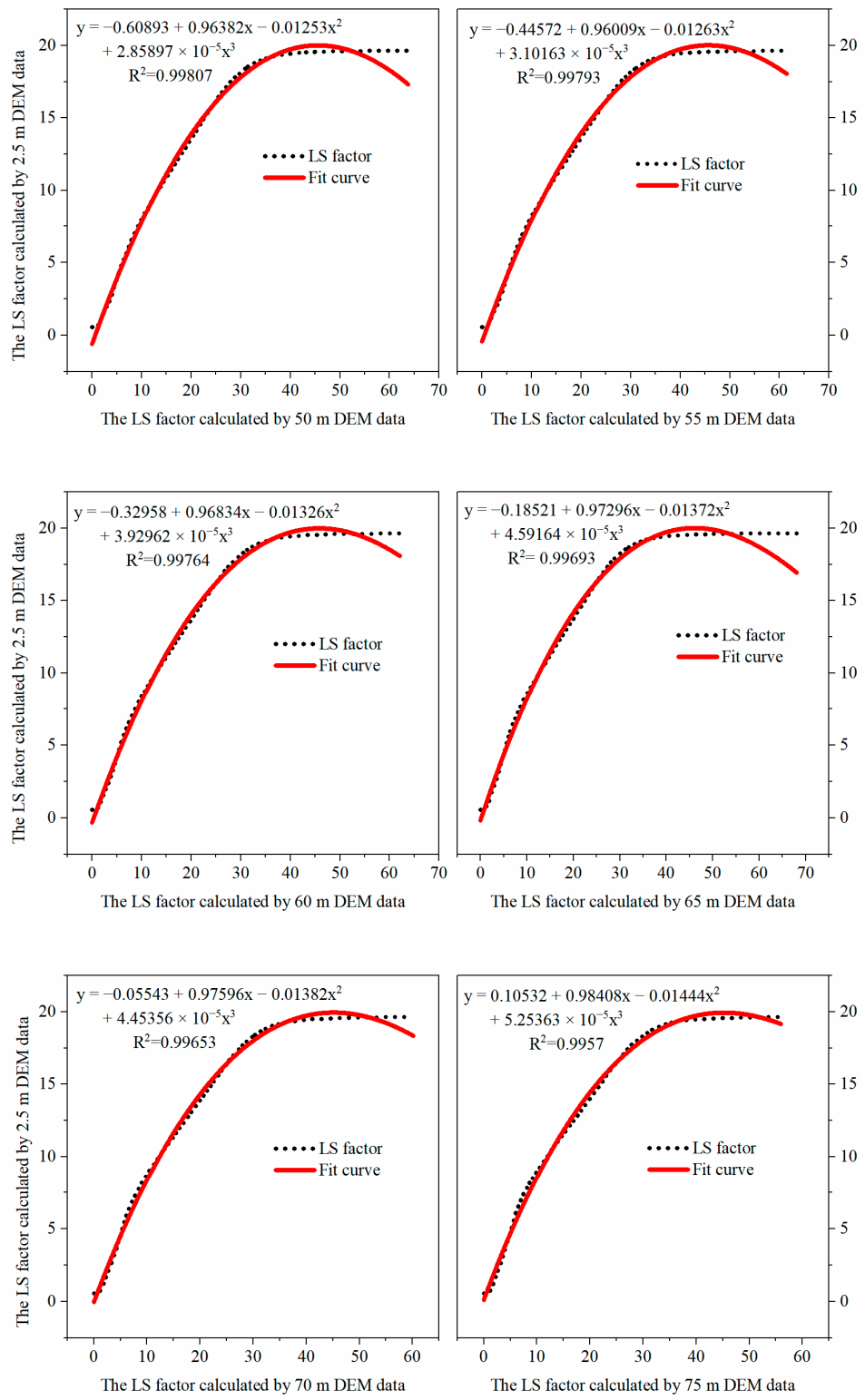


Figure 15. *Cont*.

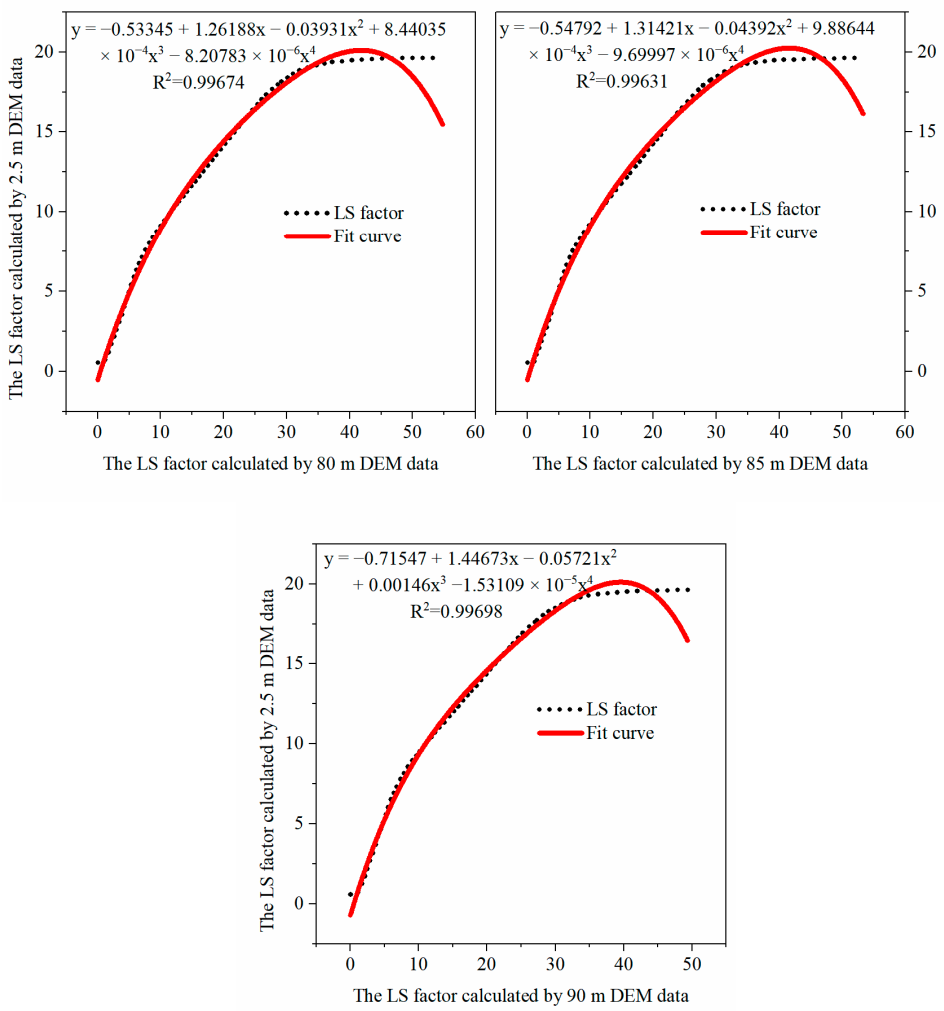


Figure 15. LS factor scale transformation model.

3.4. LS Factor Downscaling Effect

Soil erosion results before and after the downscaling of the LS factors in the Lizixi watershed were calculated from the CSLE model, as can be seen from the plot of the differences between the eroded area under low- and high-resolution DEM data before and after the downscaling (Figure 16). After the downscaling, the overall soil erosion area calculated by the low-resolution DEM data is closer to that calculated by the 2.5 m high-resolution DEM data, but the difference between the areas calculated by the 5 m and 7.5 m DEM data is slightly larger than that calculated by the pre-transformation. After downscaling, the soil erosion results at 50 m DEM were closest to the erosion results at 2.5 m high-resolution DEM data, with an area difference of only 0.39 km^2, and the maximum area difference was only 11.81 km^2, which was much smaller than that before the scale transformation. The distribution map of soil erosion intensity after scale transformation (Figure 17) shows that the spatial distribution of erosion intensity in the watershed is more consistent and closer to the soil erosion intensity calculated by 2.5 m DEM data.

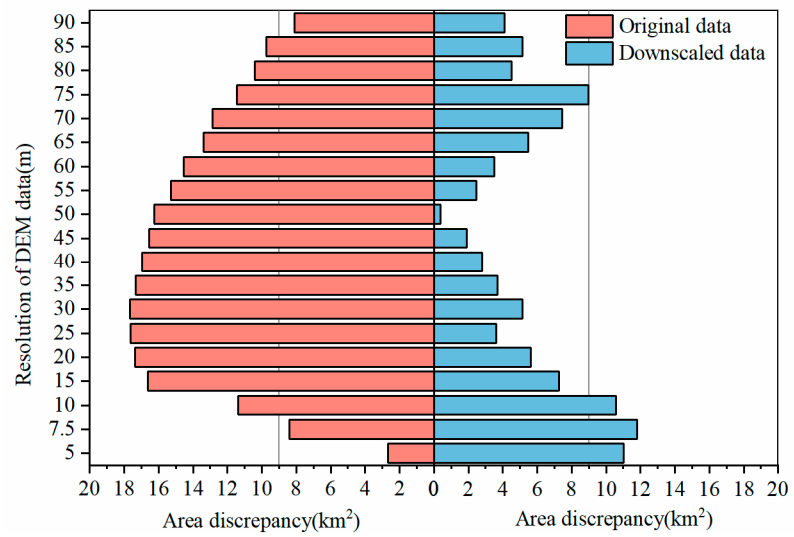


Figure 16. Erosion area difference before and after scale transformation.

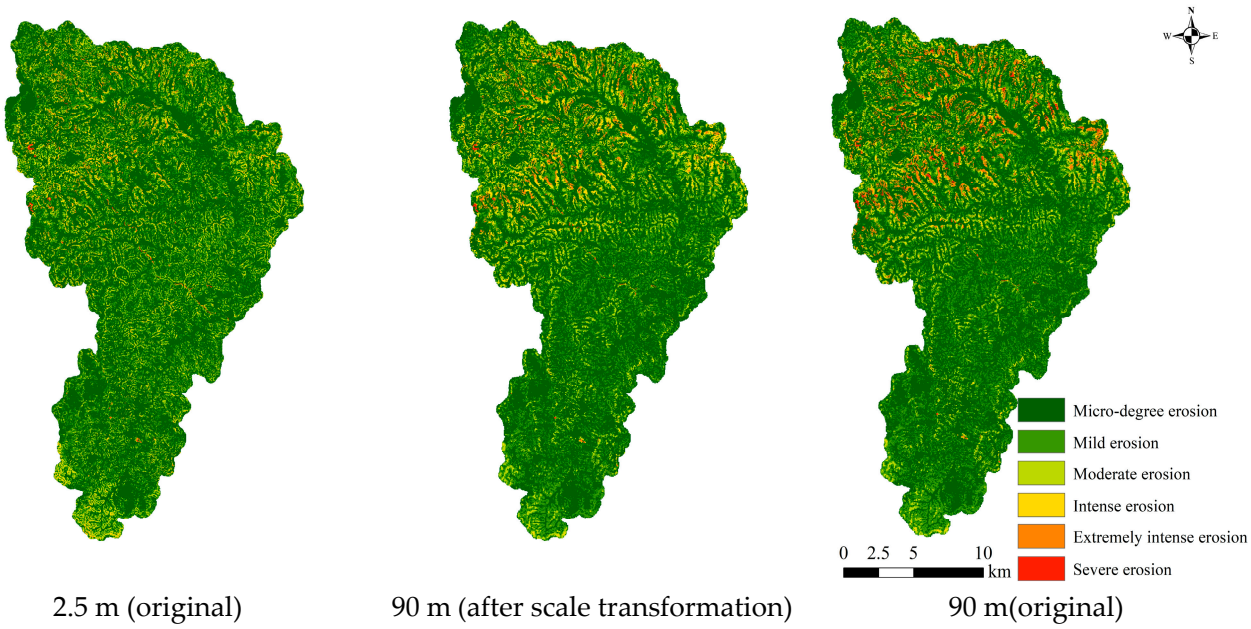


Figure 17. Distribution of soil erosion intensity after scale transformation.

4. Discussion

Slope length is a crucial factor in assessing soil erosion and has a significant role in processes such as soil erosion, transport, and deposition. The slope length is determined by truncating it when a ditch is encountered. Calculating the distribution of the ditch is crucial in determining the slope length. DEM is commonly used to extract the slope length. The location of the ditch's head is challenging to determine, so it is typically achieved by calculating the contributing area and setting a threshold to achieve a more precise slope length [25]. While there is arbitrariness and subjectivity in the threshold setting, how to determine the optimal contributing area threshold is the focus of this study. The purpose of this study to set the threshold variation in the contributing area based on the number of rasters rather than a fixed area to both take into account the resolution characteristics of the DEM itself and to provide the convenience of area setting, which is consistent with previous studies [18]. In this study, the mean values of slope lengths calculated by DEM data at different resolutions showed a tendency to increase and then stabilize with an increase in the contributing area threshold, which is consistent with the results of previous studies [3].

The contributing area threshold set in this study has a larger interval of variation than the contributing area threshold set in the previous study, which may account for the difference in the magnitude of the mean value of the slope length at stabilization. Nevertheless, the results of the two overlapping intervals are the same, suggesting that the conclusions of this study are more reliable. The determination of the optimal contributing area threshold in this study refers to the threshold-value-taking method in the extraction of the river network in the previous study; although the required results of the two are different, they are still essentially based on the DEM extraction of the ditch river network. Moreover, the trend of the contributing area threshold with river network density in the previous study is consistent with the trend of the contributing area threshold with the LS factor in this study. The application of the mean-variable-point method is also widely recognized, so both the method and the conclusion have a certain degree of credibility [17,26]. Meanwhile, this study combined the topographic characteristics of the study area to formulate the relationship between DEM resolution and the optimal contributing area threshold, which can provide new directions and ideas for research related to topographic factors and soil erosion.

In geography, scale is broadly defined to include map extent, map scale, and resolution [27]. In this study, "scale" refers to the resolution of DEM data, and the scale effect of topographic factors refers to the change in topographic factors with a change in the resolution of DEM data. Scholars from various countries have shown that the terrain attribute values extracted based on DEM data are significantly affected by the resolution of the DEM data [28–31], for example, it has been reported that when different resolutions of DEM data are selected for different geomorphology types (10–1000 m), the average slope length decreases with an increase in the DEM raster size, and the rate of decrease ranges from 0.01 to 0.06°/m [32,33]. Meanwhile, it has also been reported that [34] the estimated slope length tends to rise as the DEM raster size increases, with the rate of increase ranging from 0.6 to 2.4 m/m. In a previous study, DEM data at 2–30 m resolution with a spacing of 1 m were generated using 1:2000 digital line drawings. The results showed that the DEM grid size had different effects on the topographic factors; as the size of the DEM grid increased, the mean slope factor decreased, and the mean slope length factor increased [2]. The results of this study show that the mean value of slope decreases with a decrease in DEM data resolution, and as DEM data resolution decreases, the mean value of the slope length increases, and the change rule is consistent with previous studies. While the change in the LS factor in this study showed the trend of increasing first and then decreasing, the reason may lie in the opposite pattern of change in slope length, and the trend of the product depends on the range of the data values of slope factor and slope length factor in the study area. The mean and standard deviation rate of change results show that, when the resolution of the DEM data changes, the rate of change of these terrain elements increases and then decreases. Before the turning point, there is a significant change in the terrain elements, and the values of the elements are dispersed with a large difference, while after the turning point, there is a small change in the terrain elements, and the values of the elements are more aggregated with a smaller difference.

In this study, a terrain factor downscaling model was established based on the histogram matching principle, and from the factor perspective, the downscaling model can effectively offset the attenuation or expansion of the terrain factor, and the simulation effect is better; the results obtained by bringing it into the model show that the conversion effect is better on the whole, and the accuracy has been greatly improved compared with that before the conversion (Figure 18). However, the simulation results of the downscaling model for soil erosion results corresponding to the DEM with resolutions of 5 m and 7.5 m are poor. This could be because the 2.5 m resolution of the DEM and these two resolutions of the DEM contain closer topographic information. It is not advised to scale convert high-resolution terrain factors because the downscaling model's error is greater than the topographic information paucity of the DEM.

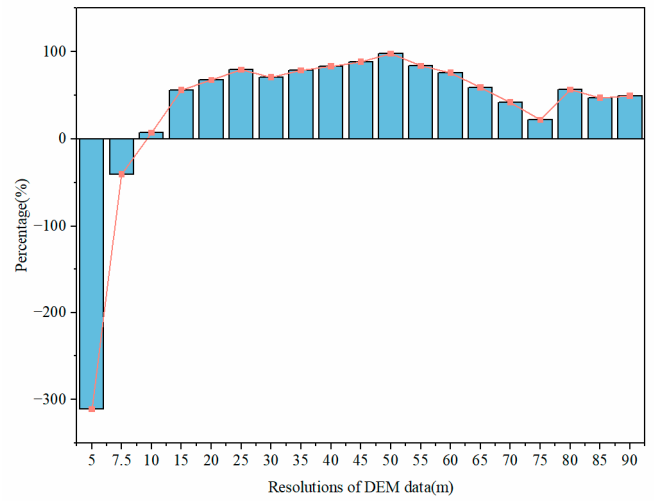


Figure 18. Percentage change in accuracy after downscaling.

5. Conclusions

(1) Based on the graph of the change rule of the mean value of the LS factor with the threshold of the contributing area at different resolutions in the study area, it can be seen that the LS factor calculated by the DEM at each resolution shows a tendency of increasing and then gradually stabilizing. The mean-variable-point approach uses this law to estimate the appropriate contributing area threshold for each resolution. In order to offer a reference for the research of the contributing area threshold, we simultaneously developed the relationship equation between the resolution of DEM data and the optimal contributing area threshold for small watersheds in hilly areas of purple soil.

(2) As the resolution of DEM data decreases, slope, slope length, and the LS factor show different scale effects. In the study area, the scale effect of the LS factor has resulted in the largest difference in soil erosion area, reaching 4.16% of the watershed area, so the scale effect of topographic factors cannot be ignored when conducting erosion investigation and evaluation.

(3) Due to the fragmented landmass within the small watersheds in the hilly area of purple soil, the lower-resolution DEM data responded to very limited topographic information. To accurately reflect the real topographic information of the study area, and to accurately calculate the results of soil erosion, we applied the histogram matching principle to the scale transformation of the LS factor, so that the LS factor computed by the low-resolution DEM data can also effectively express the information of the LS factor computed by the high-resolution DEM data. To verify the effect of the downscaling model, we substitute the transformation relationship into CSLE to calculate the soil erosion intensity. The results show that the downscaling model of the LS factor established in this study has a good simulation effect, which can provide technical support for related research of small watersheds in hilly areas of purple soil.

Author Contributions: Conceptualization, R.C., Y.Z. and A.W.; methodology, R.C. and A.W; formal analysis, R.C. and Y.Z.; investigation, R.C., J.Z., S.H. and J.L.; software, R.C. and P.L.; writing—original draft, R.C. All authors have read and agreed to the published version of the manuscript.

Funding: This research was funded by the Power Construction of China grant number (P60224) and National Key R&D Program of China (2016YFC0402301-02).

Data Availability Statement: The data presented in this study are available on request from the corresponding author. The data are not publicly available due to privacy.

Conflicts of Interest: Author Ruiyin Chen, Yonggang Zhu, Jun Zhang, Shudong Hu, Jun Luo and Peng Li were employed by the company POWERCHINA Chengdu Engineering Corporation Limited. The remaining authors declare that the research was conducted in the absence of any commercial or financial relationships that could be construed as a potential conflict of interest.

References

1. Fu, S.; Liu, B.; Zhou, G.; Sun, Z.; Zhu, X. Calculation tool of topographic factors. *Sci. Soil Water Conserv.* **2015**, *13*, 105–110.
2. Fu, S.; Cao, L.; Liu, B.; Wu, Z.; Savabi, M.R. Effects of dem grid size on predicting soil loss from small watersheds in china. *Environ. Earth Sci.* **2015**, *73*, 2141–2151. [CrossRef]
3. Lin, D.; Yu, X.; Fu, S.; Wu, S. Effect of contributing area threshold on the evaluation of soil erosion. *J. Soil Water Conserv.* **2018**, *32*, 61–67+73.
4. Li, A.; Zhang, X.C.; Liu, B. Effects of dem resolutions on soil erosion prediction using chinese soil loss equation. *Geomorphology* **2021**, *384*, 107706. [CrossRef]
5. Guo, W.; Fan, Y.; Yang, Q. Statistical distribution of slope length derived from dem with different spatial resolutions. *Res. Soil Water Conserv.* **2019**, *26*, 72–76+85.
6. Fu, S.; Wu, Z.; Liu, B.; Cao, L. Comparison of the effects of the different methods for computing the slope length factor at a watershed scale. *Int. Soil Water Conserv. Res.* **2013**, *1*, 64–71.
7. Liu, H.; Yang, Q.; Wang, C.; Li, J. Changes of dem-derived slope with horizontal resolution and their spatial distribution. *Geomat. Inf. Sci. Wuhan Univ.* **2012**, *37*, 105–109.
8. Tang, G.; Zhao, M.; Li, T.; Liu, Y.; Xie, Y. Modeling slope uncertainty derived from dems in loess plateau. *Acta Geogr. Sin.* **2003**, *58*, 824–830.
9. Wolock, D.M.; Mccabe, G.J. Differences in topographic characteristics computed from 100- and 1000-m resolution digital elevation model data. *Hydrol. Process.* **2000**, *14*, 987–1002. [CrossRef]
10. Yang, L. Ls Factor Scacle Transform and Application in Soil Erosion Sampling Survey. Master's Thesis, University of the Chinese Academy of Sciences, Beijing, China, 2020.
11. Zhang, S.; Hou, X.; Wu, C.; Zhang, C. Impacts of climate and planting structure changes on watershed runoff and nitrogen and phosphorus loss. *Sci. Total Environ.* **2020**, *706*, 134489. [CrossRef]
12. Yun, Z.; Lin, W. Runoff and sediment simulation in purple hilly area based on swat model. *J. Geo-Inf. Sci.* **2013**, *15*, 401–407.
13. Chen, R.; Yan, D.; Wen, A.; Li, C.; Shi, Z. Research on soil erosion in key prevention and control region of soil and water loss based on gis/csle in sichuan province. *J. Soil Water Conserv.* **2020**, *34*, 17–26.
14. Zhang, H.; Yang, Q.; Li, R.; Liu, Q. Estimation methods of slope gradient and slope length in watershed based on gis and multiple flow direction algorithm. *Trans. Chin. Soc. Agric. Eng.* **2012**, *28*, 159–164.
15. Zhang, H. Extraction and Analysis on Distributed Erosion Slope Length in Watershed Scale. Ph.D. Thesis, Northwest A&F University, Xianyang, China, 2012.
16. Xiang, J. *Statistical Methods for Data Processing in Nonlinear Systems*; Science Publishing House, Science Press: Beijing, China, 2000.
17. Liang, B.; Xu, Y.; Bai, L.; Luo, M.; Zhao, W. Comparison of the determination of optimal convergence threshold based on mean change-point and bifurcation ratio. *Chin. Agric. Sci. Bull.* **2017**, *33*, 76–82.
18. Chang, Z.; Jian, W.; Bai, S.; Zhang, Z. Determination of accumulation area based on the method of applying mean of change-point analysis. *J. Nanjing Norm. Univ. Nat. Sci. Ed.* **2014**, *37*, 147–150.
19. Han, L.; Rui, X.P.; Liang, H.D.; Bi, X.L.; Yang, Z.X.; Jin, L. Extraction of drainage network in three gorge reservoir area based on mean change point method. *Sci. Surv. Mapp.* **2012**, *37*, 173–175.
20. Yang, Q.; Jupp, D.; Rui, L.I.; Wei, L. Re-scaling lower resolution slope by histogram matching. In *Advances in Digital Terrain Analysis*; Springer: Berlin/Heidelberg, Germany, 2008.
21. Dai, Q.; Zhu, L. Research on the method for determining the threshold of optimal catchment area based on dem. *China Water Transp.* **2018**, *18*, 166–168.
22. Kong, F.; Li, L. Determination of river drainage area threshold for extraction of drainage network by dem. *Water Resour. Power* **2005**, *23*, 65–67+93.
23. Fan, Y.; Guo, W.; Jiang, W.; Xiang, T.; Zhao, L. Changes of derived distributed erosion slope length with dem resolution. *Yellow River* **2019**, *41*, 78–82.
24. Kuang, G.; Liu, C.; Yu, G.; Wang, J.; Zhang, G.; Wu, G. A study of differences between soil erosion classification and grading criteria and RUSLE modeling. *Pearl River* **2014**, *35*, 15–18.
25. Zhang, H.; Yang, Q.; Wang, M.; Jin, B.; Wang, L.; Li, R. Effect of channel networks cutoff on extraction of distributed erosion slope length. *J. Hydraul. Eng.* **2017**, *48*, 568–575.
26. Zhu, M.; Zhang, J.; Ma, H.; Zhu, L. Analysis of relief amplitude based on dem and the mean change-point analysis method in funiu mountain area. *J. Henan Univ. Nat. Sci.* **2020**, *50*, 36–43.
27. McVicar, T.; Davies, P.; Yang, Q.; Zhang, G. An introduction to temporal-geographic information systems (tgis) for assessing, monitoring and modelling regional water and soil processes. *Reg. Water Soil Assess. Manag. Sustain. Agric. China Aust.* **2002**, 205–223.
28. Mukherjee, S.; Mukherjee, S.; Garg, R.D.; Bhardwaj, A.; Raju, P. Evaluation of topographic index in relation to terrain roughness and dem grid spacing. *J. Earth Syst. Sci.* **2013**, *122*, 869–886. [CrossRef]
29. Lin, S.; Jing, C.; Coles, N.A.; Chaplot, V.; Moore, N.J.; Wu, J. Evaluating dem source and resolution uncertainties in the soil and water assessment tool. *Stoch. Environ. Res. Risk Assess.* **2013**, *27*, 209–221. [CrossRef]
30. Li, M.; Zhao, Y.; Gao, G.; Ding, G.; Na, Y. Effects of dem resolution on the accuracy of topographic factor derived from dem. *Sci. Soil Water Conserv.* **2016**, *14*, 15–22.

31. Yang, Z. A study on the uncertainty of extracting terrain factors from dem with different spatial resolutions: A case study of the huanwan planning area in quanzhou city, fujian province. *NanFang GuoTu ZiYuan* **2021**, 45–48.
32. Gao, J. Resolution and accuracy of terrain representation by grid dems at a micro-scale. *Int. J. Geogr. Inf. Sci.* **1997**, *11*, 199–212. [CrossRef]
33. Thompson, J.A.; Bell, J.C.; Butler, C.A. Digital elevation model resolution: Effects on terrain attribute calculation and quantitative soil-landscape modeling. *Geoderma* **2015**, *100*, 67–89. [CrossRef]
34. Wang, F.; Wang, C.M. Research for the influences of dem resolution on topographical factors—A case study of mengyin county. *Res. Soil Water Conserv.* **2009**, *16*, 225–229.

Disclaimer/Publisher's Note: The statements, opinions and data contained in all publications are solely those of the individual author(s) and contributor(s) and not of MDPI and/or the editor(s). MDPI and/or the editor(s) disclaim responsibility for any injury to people or property resulting from any ideas, methods, instructions or products referred to in the content.